Presented at the 33rd European PV Solar Energy Conference, 25-29 September 2017, Amsterdam, The Netherlands

ON THE DETERMINATION OF THE CONTACT RESISTIVITY FOR PASSIVATING CONTACTS USING 3D SIMULATIONS

Gamze Kökbudak[1,2], Ralph Müller[1, 3], Frank Feldmann[1, 3], Andreas Fell[1], Raşit Turan[2], Stefan W. Glunz[1, 3]
[1]Fraunhofer Institute for Solar Energy Systems, Heidenhofstr. 2, 79110 Freiburg, Germany
[2] The Center for Solar Energy Research and Applications (GÜNAM), Middle East Technical University, Dumlupınar Bulvarı 1, 06800 , Ankara, Turkey
[3] Laboratory for Photovoltaic Energy Conversion, University Freiburg, Germany

ABSTRACT: Besides surface passivation, a low contact resistivity is one of the most important requirements of passivating contacts in order to achieve good carrier selectivity. In this work, different methods to determine the contact resistivity were performed and compared using a passivating contact structure consisting of poly silicon on a thin silicon oxide. As the traditional 1D Transmission Line Model (TLM) includes many assumptions that are not valid for complicated structures and even the application of the analytical 2D TLM is limited, especially for very low contact resistivity values, 3D numerical simulations with Quokka3 were carried out to accurately model passivating contact structures and determine the contact resistivity by comparison to electrical measurements. The investigated sample showed both, good passivation quality with implied open-circuit voltage iV_{oc} of 716 mV together with a low specific contact resistivity of 0.21 mΩ·cm^2 as extracted from the numerical simulations. Using our method, it is possible to distinguish the sources of the contact resistivity. A fraction of 0.11 mΩ·cm^2 could be attributed to the interface between metal & poly-Si layer and 0.10 mΩ·cm^2 results from the interface between poly-Si layer & bulk.
Keywords: Passivating contact, specific contact resistivity, transfer length method, numerical simulations, Quokka

1 INTRODUCTION

Passivating contacts are a key ingredient to further push the efficiency of silicon solar cells. In the past few years, there has been a growing interest in passivating contact structures which feature an ultra-thin silicon oxide layer and a heavily doped silicon layer (TOPCon [1], poly-Si [2] or POLO [3]). Recently, solar cells have achieved efficiencies greater 25% using a passivating rear contact [4]. Moreover, SunPower is using passivating contacts for their highly efficient interdigitated back contact solar cells [5].

To obtain highly efficient passivating contacts, the recombination at the contacts needs to be minimized in order to get a high internal voltage (iV_{oc}). Additionally, the requirement of carrier selectivity can be fulfilled by allowing one type of charge carrier while blocking the other type which is necessary to obtain a high external open circuit voltage (V_{oc}). To fulfill these requirements, the structure is generally created by depositing a thin interface oxide layer and a conductive thin film on the silicon wafer. So this structure has not only several layers but also several interfaces differently from traditional solar cell structures featuring only diffused regions. In order to obtain a high fill factor (FF) from such a cell, having low contact resistivity is a necessity.

The *contact resistivity* ρ_c (Ω·cm^2), sometimes called *specific contact resistance* or *specific contact resistivity* characterizes the contact independent of the contact area [6]. For traditional silicon solar cells like diffused emitter Al-BSF cells, a low contact resistivity can be usually achieved simply by a stronger doping. However, when it comes to passivating contact cell structure which has many different layers and interfaces, the contact resistivity depends on many parameters. For solar cell designs employing localized contacts, very low contact resistivity values down to 1 mΩ·cm^2 may be needed. Hence it is very important to determine the contact resistivity of passivating contact systems accurately in a wide range.

Fig.1a shows a simple diffused emitter structure with conventional “Transfer Length Method” metal pads, which can be evaluated with the simple one-dimensional (1D) Transmission Line Model (TLM) to obtain the contact resistivity values [7-8]. In contrast, Fig.1b shows a passivating contact with the metal pattern on top of it. As the passivating contact structure includes several conductive layers and a thick bulk, there are many current paths which make the analysis of the contact resistivity more complicated. There is no existing simple evaluation method for such a case. Vertical measurement from front through the bulk to the back side works by measuring the sum of the all the ρ_c values even without current crowding effect near the metal edges as can be seen in Fig 1c. However, this method is only useful for a limited ρ_c range as the bulk resistance dominates the overall resistance when it comes to very low contact resistivity values.

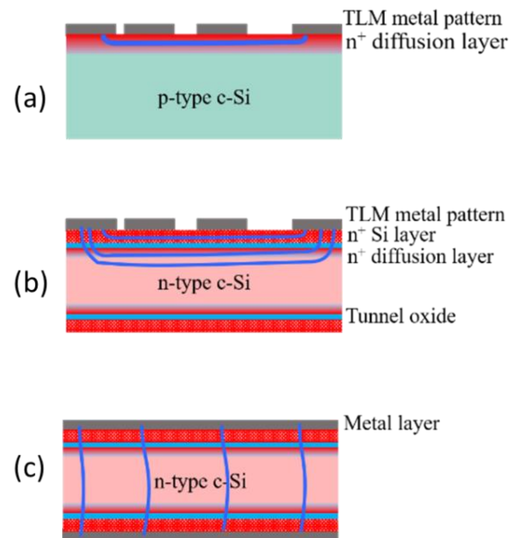

Figure 1: Schematic of the Transfer Length Method (TLM) measurement samples. Diffused emitter structure with a 1D current path (a), Passivating contact structure with many interfaces and complicated current paths (b), Passivating contact structure with vertical current flow through silicon bulk (c)

This paper focuses on the comparison of different analytical methods and uses a rigorous numerical simulation approach to accurately determine the contact resistivity accurately for complicated structures such as passivating contacts.

2 EXPERIMENTAL

n-type floating zone silicon wafers with 1 Ω·cm base resistivity and 200 µm thickness were used. After RCA cleaning, an ultra-thin silicon oxide layer was formed using the nitric acid oxidation of Si (NAOS) method on both sides. Subsequently, about/approx. 40 nm thick amorphous silicon layers were deposited by the Low Pressure Chemical Vapor Deposition (LPCVD) technique symmetrically on both sides. Subsequently, Phosphorus ion implantation was carried out with a dose of 1.5×10^{15} cm^{-2}. Then, the samples were annealed in a tube furnace at 850 ºC to activate dopants and crystallize the Si layer simultaneously. Thereafter, a remote plasma hydrogen passivation (RPHP) was applied at 400ºC for 30 min to further reduce interface recombination. The samples were prepared symmetrically to obtain Quasi Steady State PhotoConductance (QSSPC) and TLM measurements at exactly the same location on the same sample.

The passivation quality was characterized using the QSSPC technique. Next, this sample was prepared for contact resistivity measurements by defining a TLM pattern with evaporated Ti/Pd/Al stack via a photolithographical lift-off process. Finally, the resistance R as a function of the pad spacing d was determined via four probe measurements to carry out further evaluations of the contact resistivity.

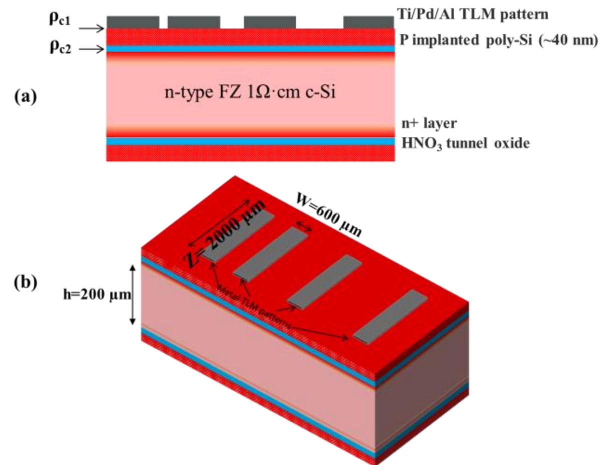

Figure 2: Cross section (a) and the isometric view (b) of the investigated symmetrical passivating contact structure

For the TLM structure, metal pad lengths of 2000 µm and widths of 600 µm were used. The spacing between metal pads increases from 20 µm to 240 µm.

For the numerical method that was proposed in this work, additional resistance obtainment via four probe measurements was carried out after implementing plasma etching process using SF_6 as a reactant gas, to remove the conductive layers in-between the metal pads on the front side of the sample (see Fig. 3).

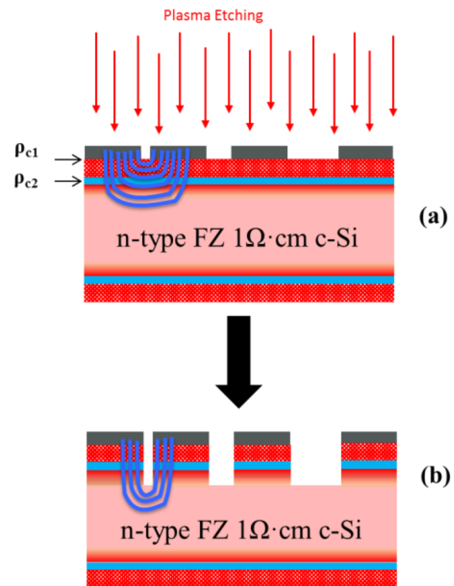

Figure 3: Passivating contact experimental structure and schematic current flow before plasma etch (a), after plasma etch (b)

3 RESULTS AND DISCUSSION

3.1 Analytical 1D-Transmission Line Model (TLM)

The contact resistivity can be obtained using the simple one-dimensional (1D) TLM, for the samples which have only one conductive layer (of very small thickness) and one interface. For this model, the total resistance is measured for various metal spacing and created as an $R(d)$ plot as can be seen in Figure 5. Non-linearity occurs for very small metal pad distances due to 2D current flow in the bulk [9]. By fitting in the linear region, some parameters can be extracted such as contact resistance R_c, sheet resistance R_{sheet} and transfer length L_T using a simple analytical theory of TLM with many assumptions that are not compatible with the complicated structures such as passivating contacts. Then, the contact resistivity value can be calculated using the extracted parameters from this plot.

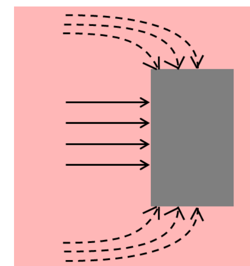

Figure 4: Current trails from the edges of the metal

The assumptions include counting only the 1D current flow by disregarding the current flowing through bulk as this model was developed only for very thin conductive layers. Current trails from the edges of the metal are also ignored (see Fig 4.) which could be avoided by cutting the sample at the edges of the metal pads. However, this may cause other problems since this

technique can introduce shunts at the cut planes and needs some additional technological effort. In the 1D TLM, all conductive layers such as doped poly-Si, the n^+ diffusion from the poly-Si into the bulk, and the bulk are all regarded as one effective layer. Another assumption is coming from the influence of the interfaces since this evaluation method includes only one "effective" interface. Furthermore, the metal layer resistance is disregarded.

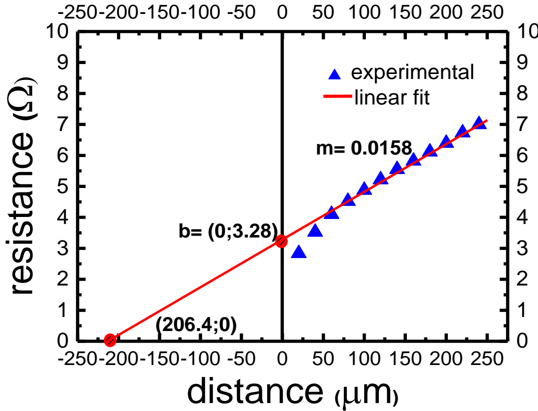

Figure 5: Plot of the measured total resistance as a function of distance between metal pads

Figure 5 shows the plot of the measured total resistance as a function of metal gap distance together with a linear fit for pad distances > 100 µm with interception points on x & y axes as well as the slope. The 1D TLM evaluation was carried out according to Equation (1) to (3). This gives the sheet resistance while transfer length L_t could be calculated from the solution of Equation (2). Here, the transfer length refers to the distance which most of the current transfers from semiconductor into metal and vice versa [10]. Finally, ρ_c could be determined as **3.45 mΩ·cm²** for this specific sample using Equation (3).

$$R_{sheet} = m \times Z = 31.6\ \Omega/\square \qquad (1)$$

$$R_C = \frac{R_{sheet}\, L_t}{Z} \coth\left(\frac{W}{L_t}\right) \qquad (2)$$

Solve for L_t:

$$L_t = 105.2\ \mu m$$

$$\rho_c = R_{sheet} \times {L_t}^2 \qquad (3)$$

Solve for ρ_c:

$$\rho_c \approx 3.45\ m\Omega{\cdot}cm^2$$

3.2 2D Analytical TLM evaluation

As the 2D current transport through the bulk of the silicon is neglected in standard 1D TLM evaluation, Eidelloth and Brendel proposed an analytical expression for the extraction of the contact resistivity from TLM measurements considering the 2D current flowing through the bulk [11]. Although this method stands for correcting the 2D bulk effect, it does not include a lateral edge effect correction (see Fig. 4). Furthermore, this method is not suitable for the structures having more than one conductive layer and several interfaces. So the highly doped poly-Si and the n^+ layer below the thin oxide are not taken into account and the contact resistivity of all interfaces is lumped together. The metal layer is also assumed to be infinitively conductive as in 1D TLM. Moreover, it was already stated that this 2D model is not applicable for small contact resistivity values such as $\rho_c \ll 1\ m\Omega{\cdot}cm^2$ [11].

From the linear fit to the measured data shown in Fig.5, the ratio of intersection with the y-axis and slope (b/m) was extracted. Using Equations (4), (5), (6) and (7), equation (8) was solved to extract ρ_c according to Ref [9]. This 2D TLM evaluation yields a contact resistivity value of **1.39 mΩ·cm²** which is much lower than the value 1D TLM gave.

$$G_{1D_TLM} = \sqrt{\gamma}\coth(\sqrt{\gamma}) \qquad (4)$$

$$G_{CM} = 1 + \gamma + \gamma\frac{\delta}{\pi}\left(\ln 4 - \ln\left(e^{\frac{\delta}{\pi}} - 1\right)\right) \qquad (5)$$

$$\gamma = W^2\rho_b/(\rho_c h) \qquad (6)$$

$$\delta = h/W \qquad (7)$$

$$\rho_c \approx 1.39\ m\Omega{\cdot}cm^2$$

3.3 3D numerical simulations

As all the analytical models include many assumptions that are not fulfilled by investigations of complex structures, Quokka3 simulations [12] were performed to model the passivating contacts accurately. Quokka3 features a fast solver for ohmic-only carrier transport and it can account for up to two conductive layers on top of the bulk including their respective interface- (i.e. contact-) resistivities. With this, Quokka3 is well suited to simulate TLM structure on the passivating contact system. Furthermore, to account for the lateral edge effect (see Fig 4), a 3D model was used. With the 3D multi-layer model it is possible to separate $\rho_{c,1}$ and $\rho_{c,2}$ where the former stands for the contact resistivity between metal and the poly-Si layer and the latter refers to the contact resistivity between poly-Si and the n^+ layer (across the thin oxide).

The fixed simulation input parameters are bulk resistivity & thickness, the symmetrical layer structure and the metal pad geometry. The variable input parameters are the sheet resistance of the two conductive layers (poly-Si and n^+ layer) as well as the contact resistivity at each interface (metal to poly-Si and poly-Si to n^+ layer across the thin oxide). These four variable parameters were varied to find the best match between simulation and experimental data. With Quokka3 being currently restricted to two conductive layers per side, we chose to disregard the sheet resistance of the metal layer in order to be able to account for the n^+ layer below the thin oxide. This assumption is reasonable as the metal layer conductivity is very high and its effect was found to be very weak in respective simulations.

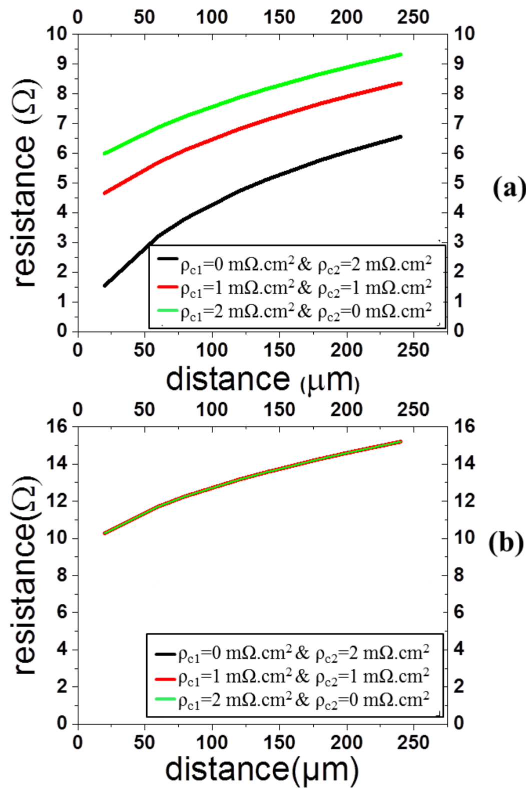

Figure 6: R(d) plots of different simulation sets created by using the fixed parameters of $R_{sheet,\ poly\text{-}Si}=10^2\ \Omega/\square$ & $R_{sheet,\ n^+\ layer}=10^2\ \Omega/\square$ (a), $R_{sheet,\ poly\text{-}Si}=10^{12}\ \Omega/\square$ & $R_{sheet,\ n^+\ layer}=10^{12}\ \Omega/\square$ (b)

Since there are four variable parameters, there may be more than one parameter set matching the experimental data. As an example, Figure 6a shows three simulations where the effective contact resistivity (sum of ρ_{c1} and ρ_{c1}) was kept constant but the contribution of ρ_{c1} and ρ_{c2} to the effective contact resistivity was varied. If the sheet resistance of the poly-Si and n^+ layer is low, the individual contributions of ρ_{c1} and ρ_{c2} have a strong influence on the total resistance (see Fig. 6a). In contrast, one cannot distinguish anymore between the contribution of ρ_{c1} and ρ_{c2} if the sheet resistances are very high (see Fig. 6b). In order to evaluate accurate values for both ρ_{c1} and ρ_{c2}, additional experimental data is needed. Therefore, plasma etching process was applied using SF_6 as a reactant gas, to remove the conductive layers in-between the metal pads on the front side (see Fig. 3) and the resistance of each structure was measured again.

Figure 3a shows the cross section of passivating contact structure and possible current paths before the plasma etching step. 4 probe resistance measurements were carried out while current is flowing from one metal pad to the second one through each of the conductive layers and through the bulk. After etching of the conductive layers between the metal pads, the current is constrained to flow from one metal contact, through all of the interfaces into semiconductor bulk and up into the second metal contact pad as shown in Figure 3b. After performing another 4 probe resistance measurement, the simulations were performed to find a unique simulation parameter set that matches both experimental data sets (before and after etch) simultaneously.

Figure 7 shows the experimental data together with the best-matching simulation parameter set.

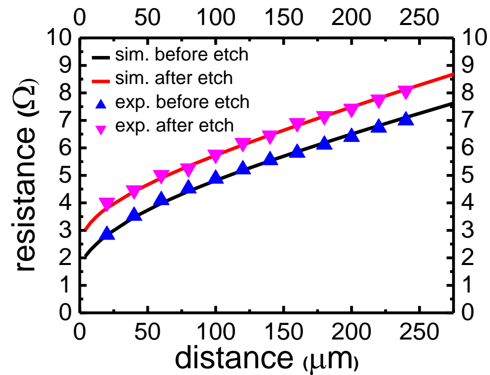

Figure 7: R(d) plot showing the best match between simulation and experimental data (ρ_{c1}=0.11 mΩ.cm^2, ρ_{c2}=0.10 mΩ.cm^2, $R_{sheet,\ poly\text{-}Si}$=15000 Ω/□, $R_{sheet,\ n^+\ layer}$=600 Ω/□)

From the simulations it was found that the investigated sample shows a contact resistivity value of **0.11 mΩ.cm²** and **0.10 mΩ.cm²** for the interfaces between metal & poly-Si (ρ_{c1}) and poly-Si & bulk (ρ_{c2}), respectively. In addition to the contact resistivity values for each interface, sheet resistances for conductive layers were found to be 15000 Ω/□ for the poly-Si layer and 600 Ω/□ for the n^+ diffused layer. Calculating the overall sheet resistance of the whole sample (parallel connection of poly-Si & n+ layer at the front and rear together with the bulk) yields 42.6 Ω/□. This value is very close to the overall sheet resistance extracted from QSSPC measurements (43 Ω/□).

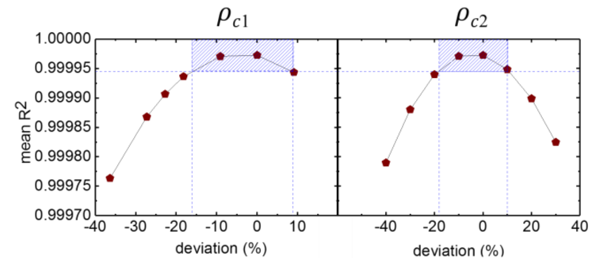

Figure 8: Sensitivity analysis on contact resistivity values (R^2 is a measure for how well simulated and experimental data match, as shown in Figure 7)

The uncertainty of the results was examined by a sensitivity analysis. A high sensitivity to ρ_c was found for both interfaces as shown in Figure 8. The shaded regions indicate the parameter range where the simulated and experimental data show a good match. For ρ_{c1}, the best match was found with 0.11 mΩ.cm^2 and the accuracy range is between 0.09 and 0.12 mΩ.cm^2. For ρ_{c2}, the best match is at 0.10 mΩ.cm^2 and the acceptable range was found to be between 0.085 to 0.11 mΩ.cm^2. Therefore, there is an uncertainty of about 10% for each extracted contact resistivity value.

For the sheet resistance of the n^+ layer, the uncertainty is less than 4% (600±20 Ω/□). Only the sheet resistance of the poly-Si layer cannot be determined accurately as its conductivity is very low. A good match was obtained in the range from 10000 to 30000 Ohm/sq.

4 SUMMARY

In order to improve the cell performance, the contact resistivity has to be low and it is required to be accurately determined especially when the cell design's contact fraction is small.

Since analytical TLM evaluations (1D & 2D) are not suitable for more than one layer and interface, a numerical simulation model using Quokka3 for exact 3D modelling of the multilayer structures was employed. The 3D model was applied to a structure consisting of several layers, i.e. passivating contact structure with LPCVD deposited and ex-situ phosphorus implanted poly-Si layer on a thin silicon oxide. Table 1 shows the comparison of different methods in terms of limitations and applicability of the methods coupled with the evaluation results for the specific sample investigated in this work. It can be seen that for the structure investigated in this work the analytical models show a large error, highlighting the usefulness and necessity of the numerical simulation approach. Notably, the speed and simplicity of the Quokka3 simulations did not impose any practical limitation on its extensive application.

Table 1: Comparison of different methods to determine the contact resistivity of passivating contact structures

Evaluation Technique	1D analytical TLM	2D analytical TLM	3D numerical simulation
Limitations for passivating contacts	• Only 1D current flow • No current through the bulk • No current flow at the edges • Only one conductive layer • Only one interface • No sheet resistance of metal layer	• No current flow at the edges • Only one conductive layer • Only one interface • No sheet resistance of metal layer	• No sheet resistance of metal layer
Applicability	• 1D pad geometry • 1 conductive layer (1D) • 1 interface	• 1D pad geometry (only with large pad distance) • 1 conductive layer (bulk 2D) • 1 interface	• 2D pad geometry • 2 thin conductive layers + 3D bulk • 3 interfaces • Back side included
Respective result: Contact resistivity [mΩ.cm²]	3.45	1.39	0.11+0.10

5 ACKNOWLEGMENTS

This work has partially funded by the German Federal Ministry for Economic Affairs and Energy under grant No. 0325827B "26+" and 03225877D "PEPPER". We also thank our colleagues at Fraunhofer ISE, especially A. Leimenstoll, F. Schätzle, A. Lösel, R. van der Vossen, A. Seiler, S. Seitz for their contribution to this work.

G. Kökbudak further thanks CHEETAH project under grant No. 609788. and The Scientific And Technological Research Council Of Turkey under grant No. 114F306.

6 REFERENCES

[1] F. Feldmann, M. Bivour, C. Reichel, M. Hermle, and S. W. Glunz, "Passivated rear contacts for high-efficiency n-type Si solar cells providing high interface passivation quality and excellent transport characteristics," Sol. Energy Mater. Sol. Cells, vol. 120, pp. 270–274.

[2] Yan, D., Cuevas, A., Bullock, J., Wan, Y., & Samundsett, C. (2015). Phosphorus-diffused polysilicon contacts for solar cells. Solar Energy Materials and Solar Cells, 142, 75-82. doi:10.1016/j.solmat.2015.06.001

[3] R. Peibst et al., "A simple model describing the symmetric I–V characteristics of p polycrystalline Si/n monocrystalline Si, and n polycrystalline Si/p monocrystalline Si junctions." IEEE J. Photovoltaics, vol. 4, no. 3, pp. 841–850, 2014.

[4] Richter, A. et al. (2017). Silicon Solar Cells with Passivated Rear Contacts: Influence of Wafer Resistivity and Thickness. Freiburg, Germany: SiliconPV 2017.

[5] D. D. Smith et al., "Toward the practical limits of silicon solar cells" IEEE Journal of Photovoltaics, vol. 4, no. 6, pp. 1465–1469, 2014.

[6] D. K. Schroder & D. L. Meier (1984). "Solar cell contact resistance – A review". IEEE Transactions on Electron Devices, 31(5), 637-647.

[7] W. Shockley, A. Goetzberger, and R. M. Scarlett, "Theory and experiments on current transfer from alloyed contact to diffused layer."Appendix B of "Research and investigation of inverse epitaxial UHF power transistors," Shockley Res. Lab., Palo Alto, CA USA, Tech. Rep.AFALL TDR 64-207, 1964.

[8] H. Berger, "Contact resistance on diffused resistors," in IEEE Int. Solid-State Circuits Conf., Dig. Tech. Papers, vol. 12. Feb. 1969, pp. 160–161.

[9] R. Brendel, & S. Eidelloth (2014). "Analytical Theory for Extracting Specific Contact Resistances of Thick Samples From the Transmission Line Method.", IEEE ELECTRON DEVICE LETTERS.

[10] D. K. Schroder (2006). "Contact Resistance and Schottky Barriers. In Semiconductor Material and Device Characterization" , (pp. 127-168).

[11] M. Rienäcker, R. Peibst, & R. Brendel (2016). "Junction Resistivity of Carrier-Selective Polysilicon on Oxide Junctions and Its Impact on Solar Cell Performance", IEEE JOURNAL OF PHOTOVOLTAICS.

[12] A. Fell, J. Schön, M. C.Schubert, S. W. Glunz (2017). "The concept of skins for silicon solar cell modeling" SOLMAT.